The 8th International Conference on Jets, Wakes and Separated Flows, ICJWSF-2024
September 23-25, 2024, Firenze, Italy

Impact of unsteady inflow on the flow features of elongated rectangular cylinders

M. Morello[1], G. Lunghi[1] S. Brusco[2] A. Mariotti[1*] and M.V. Salvetti[2]

1: Dept. of Civil and Industrial Engineering, University of Pisa, Pisa, Italy
2: Faculty of Engineering, Western University, London, Canada

[*] Corresponding author: alessandro.mariotti@unipi.it

Abstract

We conduct Large-Eddy Simulations (LES) to investigate accelerating flow around rectangular cylinders with chord-to-depth ratios of 3:1 and 5:1, employing Gaussian-type accelerations as previously studied in [6] for square cylinders. Different from square cylinders, these bodies experience shear-layer separation at the upstream corners, mean-flow reattachment along the sides, and interaction between vortical structures from Kelvin-Helmholtz instability and vortex shedding. The simulations cover Reynolds numbers ranging from $Re = 17200$ to $Re = 65360$. Both rectangular cylinders exhibit consistent frequency-time cells during acceleration. For the 3:1 cylinder, the Strouhal number and crossflow-force fluctuations remain stable. In contrast, the 5:1 cylinder shows a reduction in the recirculation region size, resulting in a narrower wake, lower lift fluctuations, and higher Strouhal numbers. The mean recirculation region shortens at higher Reynolds numbers for accelerating flows compared to steady conditions. Strouhal numbers for different acceleration severities align when plotted against the Reynolds number.

Keyword:*Large-Eddy Simulations, Gaussian-type inflow acceleration, elongated rectangular cylinders, Strouhal number, crossflow force fluctuations*

1. Introduction

We investigate the high-Reynolds-number flow around elongated rectangular cylinders with different aspect ratios under time-varying inflow conditions. Specifically, we consider streamwise-to-crossflow length ratios of 3:1 and 5:1. These configurations represent simplified geometries of structures commonly found in wind engineering, such as tall buildings and bridges. Under steady inflow conditions, the flow pattern around rectangular cylinders of different aspect ratios has been widely investigated. For all aspect ratios, flow separation occurs at the upstream edges. Rectangular cylinders with small chord-to-depth ratios, such as the 2:1 ratio and square cylinders, are characterized by separated shear layers that can undergo Kelvin-Helmholtz instability and directly form the von Karman vortex street in the wake [11, 14, 16]. For larger chord-to-depth ratios (e.g., 3:1, 5:1), Kelvin-Helmholtz instability in the separated shear layers leads to the formation of vortical structures along the lateral sides of the cylinder. These structures are then convected downstream along the cylinder and interact with each other and, further downstream, with the rear edges of the cylinder, forming the von Karman vortex shedding in the wake [16]. In terms of mean flow, a closed recirculation region is found on the lateral side of the cylinder [5, 7, 10]. Many studies have identified the range $2.5 \leq B/D \leq 3$ as the cut-off between separated and attached mean flows on the cylinder lateral surface [13, 16]. In case of attached mean flows, the recirculation region occupies the entire side of the rectangular cylinder in the case of the 3:1 ratio, while it is shorter than the side for the 5:1 geometry [12, 13].

Nevertheless, civil structures are usually subject to non-stationary wind conditions due to events such as thunderstorms. Accelerating flow conditions significantly affect fluctuating loads, flow dynamics, and surface pressures [3, 4], and can cause severe damage to the structure, posing safety risks. Also under these unsteady wind condition, the chord-to-depth ratio of the rectangular cylinder ruled different dynamics for

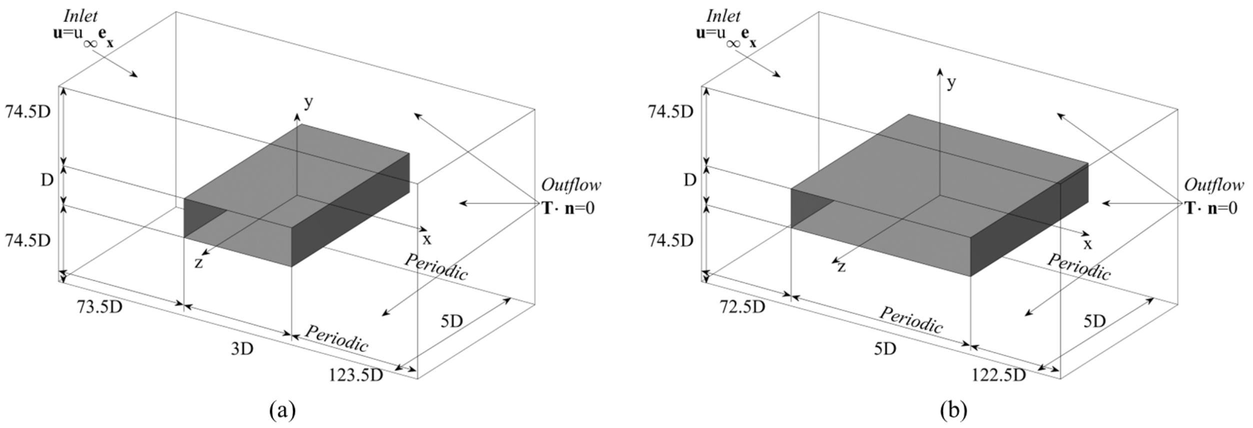

Fig. 1: (a) Sketch of the 3:1 computational domain. (b) Sketch of the 5:1 computational domain.

the separated shear layers and the wake flow [15]. For instance, experiments and Large-Eddy Simulations (LES) on accelerating and decelerating flows on square cylinders identify the presence of constant-frequency time cells during the vortex shedding from a square cylinder, leading thus to a different Strouhal number in the vortex shedding compared to the one estimated under steady flow conditions [1, 2, 8, 9]. This research activity aims to extend the investigation to rectangular cylinders with different aspect ratios under the same accelerating inflow conditions. Our goal is to determine whether the vortex shedding frequency exhibits constant-frequency time cells, as observed for square cylinders, and to understand how possible changes in the vortex shedding frequencies affect load predictions and their related fluctuations.

2. Problem definition and investigation methodology

The incompressible flow around 3:1 and 5:1 rectangular cylinders at zero angles of attack is investigated herein. LESs are conducted utilizing the open-source code Nek5000, which employs a high-order spectral-element method. Each spectral element is either rectangular or an appropriate coordinate mapping of that one. Inside these elements, the basis functions consist of Legendre polynomials of order N for velocity and $N-2$ for pressure in each direction; herein $N = 6$, consistent with [9, 15, 16]. Time advancement is achieved through a third-order backward finite-difference scheme based on the high-order splitting method. The computational domains for the 3:1 and 5:1 rectangular cylinders are illustrated in Figs. 1a and 1b, respectively. The center of the cylinder is positioned at $x/D = y/D = 0$, where D represents the cylinder crossflow dimension. The computational domains extend over the dimensions: $-75 \leq x/D \leq 125$, $-75 \leq y/D \leq 75$, and $0 \leq z/D \leq 5$.

The spectral element size and arrangement replicate those in [12]. Specifically, near the cylinder, the element size is $\Delta x/D = \Delta y/D = 0.125$ in the streamwise and crossflow directions, and uniform in the spanwise one ($\Delta z/D = 0.558$). A low-pass filter is implemented on the velocity field in the modal space to introduce a damping in the highest resolved modes, which can be seen as a subgrid-scale dissipation.

At the inlet, a spatially-uniform time-varying velocity condition is imposed, as in the simulations on the square cylinder in [8, 9]. Smooth inflow is considered (no turbulence). Figure 2 shows the time evolution

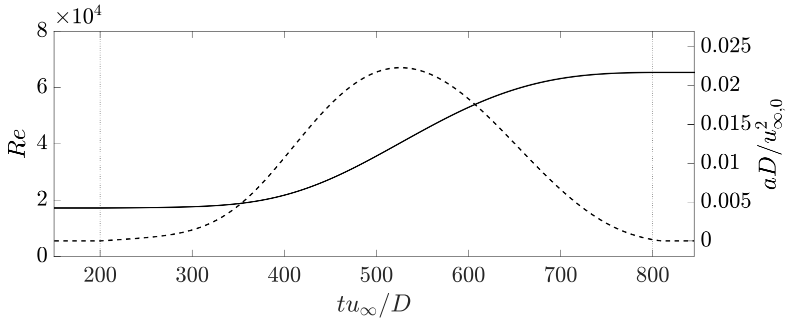

Fig. 2: Inflow Reynolds number and inflow non-dimensional acceleration.

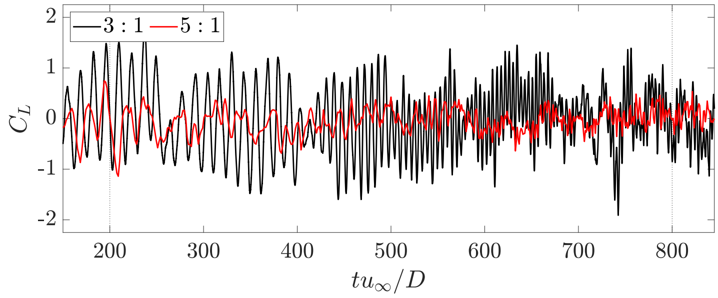

Fig. 3: Time history of the crossflow-force coefficient, C_L.

of the inflow Reynolds number, Re, and the non-dimensional acceleration normalized by the inlet velocity at $t = 0$, $aD/u^2_{\infty,0}$. The boundaries of the acceleration region, namely $tu_\infty/D = 200$ and $tu_\infty/D = 800$, are highlighted by two dotted vertical lines. The inflow Reynolds number ranges from $Re = 1.720 \times 10^4$ to $Re = 6.536 \times 10^4$, and the maximum non-dimensional acceleration reaches 2.35×10^{-2}. Moreover, traction-free boundary conditions are applied at the outflow, upper, and lower boundaries of the domain, while no-slip conditions are applied at the body surface. Periodic boundary conditions are employed in the spanwise direction.

3. Results and Discussion

Figure 3 shows the time evolution of the crossflow-force coefficients, C_L, for 3:1 and 5:1 rectangular cylinders. As can be expected, much larger oscillations are present for the 3:1 cylinder compared to the 5:1 cylinder. Moreover, as the inflow velocity increases, the time periods of the lift oscillations decrease. Figures 4a and 4b illustrate two time instants for the 3:1 rectangular cylinders at $tu_\infty/D = 401.46$ and $tu_\infty/D = 415.85$. We selected an instant when the oscillations of C_L are clearly visible (Fig. 4a) and an instant when the fluctuations of C_L significantly decrease (Fig. 4b). The spanwise component of the vorticity field clearly highlights an interruption in the alternate vortex shedding for $tu_\infty/D = 415.85$. The near wake becomes more symmetric, resulting in a significant decrease in crossflow force fluctuations. Conversely, at $tu_\infty/D = 401.46$, the alternating shedding of vortices is clearly observed. The same phenomenon occurs for the 5:1 rectangular cylinder, as seen by comparing Figs. 5a and 5b, which show two time instants at $tu_\infty/D = 494.54$ (alternate vortex shedding) and $tu_\infty/D = 502.45$ (vortex shedding interruption).

To analyze the time behavior of the characteristic frequencies, we carried out a time-frequency analysis based on the continuous wavelet transform. As in [8, 9], we adopted a complex Morlet wavelet with a central frequency of 6π. The wavelet ridges of the vortex-shedding frequency, n^*, obtained from the energy maps, are shown in Fig. 6a. Constant-frequency time cells in the vortex shedding frequency during the accelerating flow are present for both 3:1 and 5:1 rectangular cylinders. From the time behavior of the dominating frequency, n^*, we also compute the vortex-shedding Strouhal number, $St = n^*D/u_\infty$, shown in Fig. 6b. The nearly constant frequency within each cell leads to a decrease in the Strouhal number, since the inflow velocity increases. For the 3:1 cylinder, the Strouhal varies in the range $0.15 < St < 0.19$. The

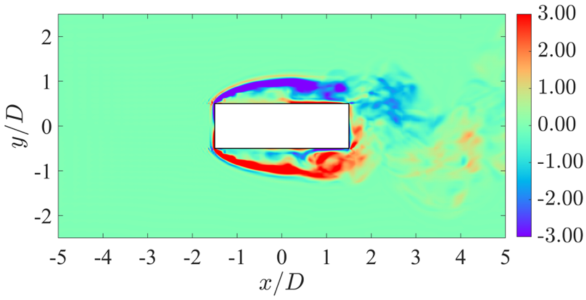

(a)

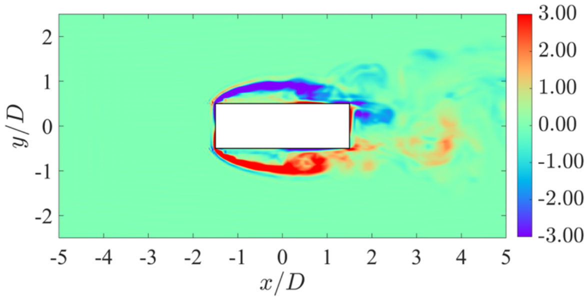

(b)

Fig. 4: Spanwise-averaged vorticity for the 3:1 rectangular cylinder at instant: (a) $tu_\infty/D = 401.46$ and (b) $tu_\infty/D = 415.85$.

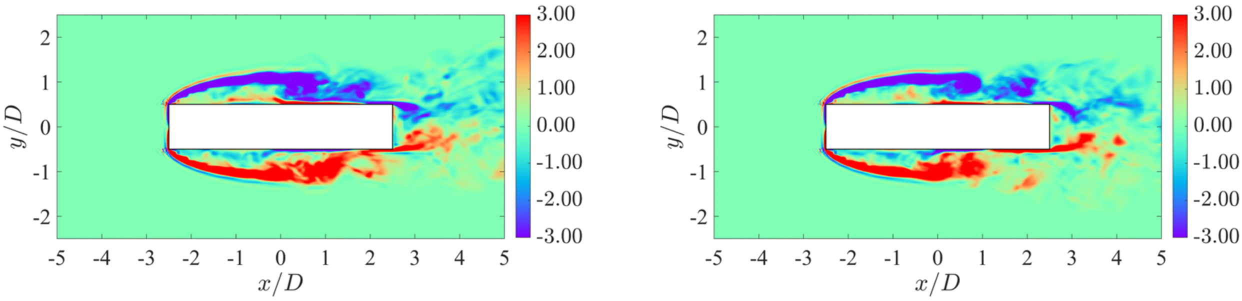

(a) (b)

Fig. 5: Spanwise-averaged vorticity for the 5:1 rectangular cylinder at instant: (a) $tu_\infty/D = 494.54$ and (b) $tu_\infty/D = 502.45$.

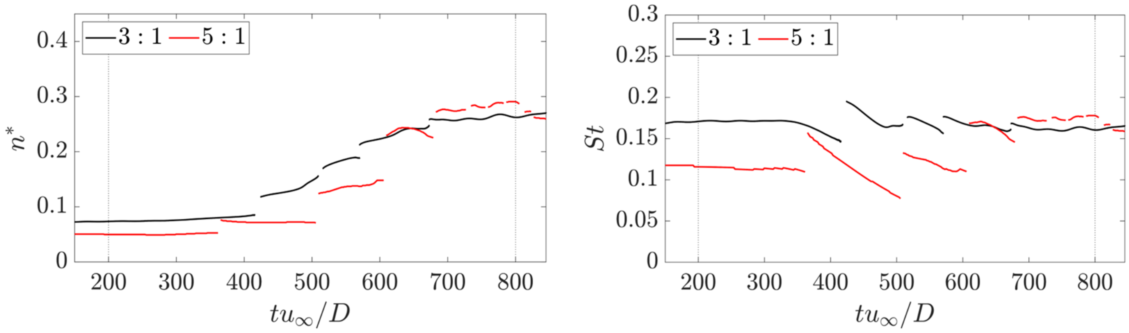

(a) (b)

Fig. 6: (a) Vortex-shedding frequency. (b) Vortex-shedding Strouhal number.

mean value of St within each cell does not change during acceleration, similar to that observed for square cylinders. On the contrary, for the 5:1 cylinder from the time-averaged statistics across different cells, with an increase in velocity, the average Strouhal number increases and the fluctuations in lift coefficient reduce. This is related with a different flow topology within each constant-frequency time cells. Indeed, the lateral mean recirculation region undergo a stepwise shortening during the accelerating flow and, thus, the averaged vortex-shedding Strouhal number within each time cell increases (as found also in [5]).

4. Conclusions

The impact of accelerating flows around 3:1 and 5:1 rectangular cylinders has been investigated using LES. In both cases, the vortex-shedding frequency shows a stepwise increase during inflow acceleration. Although the flow topology differs for elongated rectangular cylinders compared to square cylinders, constant-frequency time cells are observed, similar to those previously found for square cylinders. For the 3:1 cylinder, the Strouhal number varies between 0.15 and 0.19. The mean value of St within each cell remains constant during acceleration, mirroring the behavior seen in square cylinders. On the other hand, for the 5:1 cylinder, the time-averaged statistics across different cells show that with increasing velocity, the average Strouhal number rises, and the fluctuations in the lift coefficient decrease.

5. Acknowledgments

We acknowledge the CINECA award under the ISCRA initiative, for the availability of high-performance computing resources and support.

[1] S. Brusco et al. “Constant-frequency time cells in the vortex-shedding from a square cylinder in accelerating flows”. In: *J. Wind Eng. Ind. Aerod.* 230 (2022), p. 105182.

[2] S. Brusco et al. “Transient aerodynamics of a square cylinder under downburst-like accelerating flows reproduced in a multiple-fan wind tunnel”. In: *J. Fluids Struct.* 124 (2024), p. 104038.

[3] F. Guo et al. “Numerical investigation of flow around a square cylinder in accelerated flow”. In: *Phys. Fluids* 33 (2021), p. 104105.

[4] X. Li et al. “Study on the time-varying extreme value characteristic of the transient loads on a 5: 1 rectangular cylinder subjected to a thunderstorm-like wind”. In: *J. Wind Eng. Ind. Aerod.* 229 (2022), p. 105161.

[5] G. Lunghi et al. “Impact of the lateral mean recirculation characteristics on the near-wake and bulk quantities of the BARC configuration”. In: *Wind Struct.* 34(1) (2022), pp. 115–125.

[6] G. Lunghi et al. “Influence of inflow acceleration on the aerodynamic characteristics of a square cylinder”. In: *J. Wind Eng. Ind. Aerod.* 252 (2024), p. 105814.

[7] A. Mariotti, G. Lunghi, and M. V. Salvetti. “Experimental investigations on the effect of upstream-edge rounding on the BARC configuration”. In: *J. Wind Eng. Ind. Aerod.* 251 (2024), p. 105787.

[8] A. Mariotti et al. “Effect of inflow acceleration on a square cylinder”. In: *J. Wind Eng. Ind. Aerod.* Article in Press (2024).

[9] A. Mariotti et al. “Large-Eddy Simulations of the accelerating flow around a square cylinder”. In: *In: Marchioli, C. et al. (eds.) Direct and Large Eddy Simulation XIII, ERCOFTAC Series* 31 (2024), pp. 23–28.

[10] E. Pasqualetto et al. “Experimental characterization of the lateral and near-wake flow for the BARC configuration”. In: *Wind Struct.* 34(1) (2022), pp. 101–113.

[11] W. Rodi. “Comparison of LES and RANS calculations of the flow around bluff bodies”. In: *J. Wind Eng. Ind. Aerod.* 69 (1997), pp. 55–75.

[12] M. V. Salvetti et al. “Large-Eddy Simulations of the Flow Around Rectangular Cylinders of Different Chord-to-Depth Ratios: Impact of Upstream-Edge Sharpness”. In: *In: Marchioli, C. et al. (eds.) Direct and Large Eddy Simulation XIII, ERCOFTAC Series* 31 (2023), pp. 35–40.

[13] A. Sohankar. “Large eddy simulation of flow past rectangular-section cylinders: Side ratio effects”. In: *J. Wind Eng. Ind. Aerod.* 96 (2008), pp. 640–655.

[14] F. X. Trias, A. Gorobets, and A. Oliva. “Turbulent flow around a square cylinder at Reynolds number 22,000: A DNS study”. In: *Comput. Fluids* 123 (2015), pp. 87–98.

[15] T. Yang and M. S. Mason. “Aerodynamic characteristics of rectangular cylinders in steady and accelerating wind flow”. In: *J. Fluids Struct.* 90 (2019), pp. 246–262.

[16] D. Yu and A. Kareem. “Parametric study of flow around rectangular prisms using LES”. In: *J. Wind Eng. Ind. Aerod.* 77 (1998), pp. 653–662.